Vortex avalanches in Nb thin films: Global and local magnetization measurements

P. Esquinazi and A. Setzer
Department of Superconductivity and Magnetism, Universität Leipzig, Linnéstrasse 5, D-04103 Leipzig, Germany

D. Fuchs*
Department of Condensed Matter Physics, The Weizmann Institute of Science, Rehovot 76100, Israel

Y. Kopelevich
Instituto de Fisica, Unicamp, 13083-970 Campinas, Sao Paulo, Brazil

E. Zeldov
Department of Condensed Matter Physics, The Weizmann Institute of Science, Rehovot 76100, Israel

C. Assmann
Cryosensoric Laboratory, PTB, Abbestrasse 10-12, D-10587 Berlin, Germany
(Received 4 May 1999)

We have performed superconducting quantum interference device and μ-Hall local magnetization measurements on Nb thin films of different thicknesses ($120\,\text{nm} \leqslant d \leqslant 1200\,\text{nm}$) and widths ($95\,\mu\text{m} \leqslant w \leqslant 900\,\mu\text{m}$) in order to characterize the effects due to thermomagnetic instabilities (TMI's) and their geometry dependence. We show that the second magnetization peak which occurs at fields $H_{SMP}(T) \ll H_{c2}(T)$ depends on the sample dimensions and discuss it in terms of the classical theory of TMI's. Local magnetization measurements reveal a domelike flux profile at low fields which is not due to edge barriers. The Bean-like flux distribution is recovered at applied fields $H \geqslant H_{SMP}(T)$. [S0163-1829(99)04138-7]

I. INTRODUCTION

The motion of vortices in type II superconductors depends on the vortex-vortex interactions as well as on the interaction between them and the pinning centers. Due to pinning, an applied magnetic field H leads to a flux distribution or gradient inside the superconducting sample which can usually be well described by the Bean model.[1] Therefore, from the field dependence of the magnetization M one can obtain information on the pinning properties of the superconducting sample like, for example, the critical current density j_c. The relation between the observed field dependence of the magnetization and the pinning force implicitly assumes that the flux distribution corresponds to that of an isothermal critical state; i.e., the redistribution of flux inside the sample produced by a change of the externally applied field occurs without a global or local change in temperature T. However, the entry, exit, or redistribution (without a change in number) of vortices in the sample leads, always, to an energy release and therefore to a local or global temperature change. Under certain experimental conditions, which depend on the thermal and magnetic diffusivities and the thermal coupling of the sample with its environment, this temperature change can produce flux jumps if the critical current density $j_c(T,H)$ decreases with temperature.

The development of thermomagnetic flux-jump instabilities during flux penetration has been extensively studied in conventional and high-T_c superconductors (HTS's).[2–8] Usually, the observation and characterization of the effects produced by the thermomagnetic instabilities have been carried out measuring the flux jumps observed in magnetization measurements using a superconducting quantum interference device (SQUID) (see, for example, Ref. 9), Hall probes,[4] or even in vibrating reed measurements.[10] When flux jumps are absent, one usually assumes that thermal equilibrium is preserved. Surprisingly, the possible influence of a thermomagnetic instability, i.e., a local temperature change due to flux motion, to the field-dependent magnetization curves has not been accounted for properly in the literature. Regarding measurements of thermomagnetic instabilities in Nb we note that flux jumps at low applied fields accompanied by temperature fluctuations and vanishing of these with increasing field have been reported for a Nb crystal long ago.[11] More recently, Hall probes have been used to measure the internal field and some characteristics of vortex avalanches in a 20 μm thick polycrystalline Nb sample.[12] According to these authors the observed catastrophic avalanches at low temperatures cannot be understood within the concept of self-organized critically alone.

Recently, two of the authors of this paper have reported the existence of a ''second magnetization peak'' (SMP) in a 120 nm thick Nb film which was clearly produced by thermomagnetic instabilities.[13] The magnetization peak appears at fields higher than the first maximum observed usually in a zero-field-cooled (ZFC) state, but much lower than the upper critical field $H_{c2}(T)$. The field $H_{SMP}(T)$, at which the SMP in Nb thin films occurs, separates a flux jumping part of the magnetization curve $M(H)$ at $H < H_{SMP}(T)$ from a smooth behavior at $H > H_{SMP}(T)$. The significance of a SMP in a Nb thin film becomes clear when one realizes the striking similarity between its behavior and the one measured in Bi2212 high-T_c compounds.[13] Therefore, we think that a

careful characterization of the SMP in Nb films is important and may contribute to understanding the anomalous behavior of the magnetization curve $M(H)$ measured in high-T_c and other unconventional superconductors which in some cases is interpreted in terms of a vortex lattice phase transition.

In this work we have studied the behavior of the magnetization under the influence of flux jumps and the SMP in six Nb thin films. The studies have been done mostly with the SQUID. In one of the films [Nb4, thickness $d=(1140 \pm 40)$ nm] the local magnetization has been studied using a μ-Hall sensor array.[14,15] The following issues were investigated: (1) the geometry dependence of the SMP and to what extent the observed behavior can be understood within the TMI theories, (2) if the Bean-like profile assumed by the thermomagnetic instability (TMI) theories is realistic when vortex avalanches occur, and (3) finally, we look for a simple explanation of the temperature dependence of the field $H_{SMP}(T)$ that marks the SMP in magnetization measurements.

The results reported in this paper indicate that $H_{SMP}(T)$ increases with the thickness and/or width of the film as expected for measurements in transverse geometry. We found, however, that some of our results do not follow the predictions of a more developed theory for TMI's. Besides the clear observation of SMP's in our Nb thin films we report also on the observation of a dome shape in the field profile at low fields in Nb thin films.

The paper is organized as follows. In the next section we review the basic concepts of the theory of flux jumps including recently published theoretical work for TMI's in thin films. In Sec. III we describe the samples and other experimental details. Section IV is devoted to the presentation and discussion of the results. The conclusion is given in Sec. V.

II. STABILITY CRITERIA FOR THERMOMAGNETIC INSTABILITY

In the simple treatment of thermomagnetic instability and flux jumps without flux creep a Bean-like field profile is assumed[2,5] which changes its slope after a change of the external applied field. The penetration or exit of flux after the increase or decrease of the external field is *always* accompanied by energy dissipation and an incremental temperature change. If the critical current density decreases with temperature, the local temperature change produced by the flux movement allows an abrupt increase or decrease of the amount of flux in the sample. If the magnetic diffusion time is much shorter than the thermal diffusion time, an adiabatic heating of the superconductor occurs since no effective redistribution and removal of heat is possible.

Following the original derivation of Swartz and Bean[2] (see also Ref. 5) the critical value of the effective sample geometry above which TMI's can produce flux jumps is

$$s_{\mathrm{crit}}=\left(-\frac{10^2\pi C}{16 j_c \partial j_c/\partial T}\right)^{1/2}, \tag{1}$$

where C is the specific heat. The effective sample geometry s_{crit} coincides with the half thickness $d/2$ of a slab if the magnetic field is applied parallel to the main area of the sample. For the transverse geometry the effective size of a rectangular thin sample [$d \ll l,w$ (length, width)] can be approximated as[16]

$$s \sim (wd/2)^{1/2}. \tag{2}$$

The field at which the first flux jump occurs is

$$H_{fj}=\left(-\frac{\pi^3 C j_c}{\partial j_c/\partial T}\right)^{1/2}. \tag{3}$$

The influence of the local temperature change on the magnetization curve will dependent on different parameters such as, for example, the ratio between thermal ($\propto \kappa/C$, the ratio between thermal conductivity and specific heat) and magnetic ($\propto \rho_{FF}$, the flux-flow resistivity) diffusivities, the thermal coupling of the sample to the substrate and environment, the field rate, and the geometry of the sample, apart from the intrinsic superconducting properties of the sample like j_c.

In a recently published work Mints and Brandt[8] considered TMI's in superconducting thin films assuming the Bean critical state model in transverse geometry. The authors took also into account the thermal boundary resistance between the thin film and substrate through the parameter q. In the case of an ideal heat transfer coefficient $h \to \infty$, $q \simeq \pi/2d$. For high thermal boundary resistance $hd \ll \kappa$ and $q \simeq \sqrt{h/\kappa d}$. The authors found the following criterion for thermomagnetic flux-jump instability:

$$\frac{H_{fj}\mu_0 \dot{H} n}{\kappa q^2 j_c}\left[\frac{\partial j_c}{\partial T}\right]=1, \tag{4}$$

assuming that the instability originates at the film edge where the electric field is maximum.[8] Equation (4) determines the field at which the first flux jump occurs at the straight edges of the sample as a function of the applied field rate $\dot{H}$, the heat transfer coefficient h from the film to substrate, and the exponent $n \gg 1$ of the j-E curve, i.e., $j(E)=j_c(E/E_0)^{1/n}$. Our measurements as a function of field rate and thickness of the film will test, therefore, to what extent the theoretical framework helps us to understand the observed instabilities in Nb thin films in transverse geometry.

We would like to note that, in general, instability criteria like $s > s_{\mathrm{crit}}$, for example, provide only a parameter threshold (geometry, field rate, etc.) as an estimate for the possible existence of jumps, i.e., the critical case of instability. In principle, however, the influence of a local temperature change may be observed in samples with effective geometry smaller than the critical one and without having jumps. In this case one can in principle expect that the flux distribution in the sample shows deviation from an ideal Bean-like critical state model.

III. SAMPLES AND EXPERIMENTAL DETAILS

The Nb thin films were sputtered in an argon atmosphere at the Cryosensoric Laboratory in Berlin. The deposition was done onto an oxidized 400 nm thick undoped silicon wafer of 300 μm thickness. Part of the film was used to measure the residual resistance ratio (RRR). The thickness was measured using a Alpha-Step profilometer and also estimated from the RRR. The error bars of the thickness are the maxi-

TABLE I. Characteristics of the investigated samples. The RRR was measured between ~10 K and 300 K. Patterning procedures: ''L,'' lift-off; ''E,'' chemical etching; ''LA,'' laser ablation. The sample Nb3s consists of nine stripes obtained from structuring sample Nb3; the dimensions in the table refer to a single stripe.

Sample	thickness d (nm)	Width×length $(\mu m)^2$	Patterning	RRR
Nb0	120±10	885× 870	E	-
Nb1	380±30	900×1000	L	5.8
Nb3	770±45	900×1000	L	6.5
Nb3′	770±45	900×1000	E	6.5
Nb3s	770±45	95× 900	L, LA	6.5
Nb4	1140±40	892×1000	E	6.7
Nb9	355±15	846×1015	E	4.8

mum error covered by these two independent measurements; see Table I.

After deposition and to protect their surface the samples were covered with $\simeq 1.6\,\mu$m thick photoresist film. Sample Nb3 was further structured by laser ablation, making nine stripes of 95 μm width and 900 μm length each and separated by 15 μm (sample Nb3s). Upper and surface-superconductivity critical fields as well as other parameters of sample Nb0 were published previously.[17] The behavior of the second magnetization peak of this sample was published recently.[13] The roughness of the films is $<2-4$ nm depending on the thickness. In general, the films show a critical current density at low temperatures $j_c \sim 10^{10}$ A/m^2, and a Ginzburg-Landau parameter $\kappa \sim 10$; see Ref. 17.

Isothermal, global magnetization measurements as a function of applied field H were performed with a SQUID magnetometer (Quantum Design MPMS7) with H at various angles with respect to the main surface of the films. In this work we show the results with the field applied perpendicular to the surface.

Isothermal, local magnetization measurements have been performed on sample Nb4 using an array of 21 two-dimensional electron gas (2DEG) Hall sensors formed at a heterointerface of GaAs/AlGaAs. Each sensor has an active area of $10\times 10\,\mu$m^2 and 20 μm separation between sensor centers. The sample was positioned using a fine wire connected to a X-Y-Z micrometer stage and adhered to the surface of the array with a low-melting-temperature wax. Sensor No. 21 was placed outside of the sample and No. 1 near the middle of the sample (sample width $w \sim 900\,\mu$m). For more details on the Hall sensor array see Refs. 14 and 15.

IV. RESULTS AND DISCUSSION

A. First flux jump

In this subsection we present and discuss the field at which the first flux jump occurs. We also estimate the maximum magnetic energy which may accompany the first flux jump at H_{fj} and be dissipated in the sample. Figure 1 shows the magnetization in the ZFC state of samples Nb3′ and Nb4 at $T=6$ K. The inset shows the whole hysteresis loop for sample Nb4 where we recognize clearly the SMP at $H_{\rm SMP} = 1260$ Oe.

To estimate the maximum energy which can be dissipated at the first flux jump and the corresponding maximum temperature change we follow a similar thermodynamic analysis as in Ref. 5. The maximum energy stored is given by the area under the magnetization curve up to the field of the first magnetization maximum H_{fp}. Since the volume of the Nb sample is negligible in comparison with the substrate, for both samples of Fig. 1 and with $H_{fj}=100$ Oe we obtain $E_{\rm max} \sim 10^3$ erg/cm^3. If we assume that the thermal coupling between the substrate and Nb is perfect, we can use the specific heat of Si as a good approximation to estimate the maximum temperature increase if the stored energy is dissipated after H_{fj}. A straightforward calculation with an initial temperature of 6 K gives a final maximum temperature of 6.6 K. If we consider the limit of a high thermal resistance between Nb and substrate, we take only the volume and specific heat of the Nb film for the Nb4 sample and we obtain a maximum temperature of $T \sim 8.5$ K. Certainly, the temperature increase is much smaller because the magnetization does not vanish at H_{fj} at 6 K as we see in Fig. 1. The real temperature increase in the sample at the temperature of the measurements depicted in Fig. 1 is only a fraction of the maximum temperature increase calculated above. However, the lower the temperature and due to the decrease of the specific heat and the increase in the critical current density, the temperature increase at $H > H_{fj}$ may increase substantially.

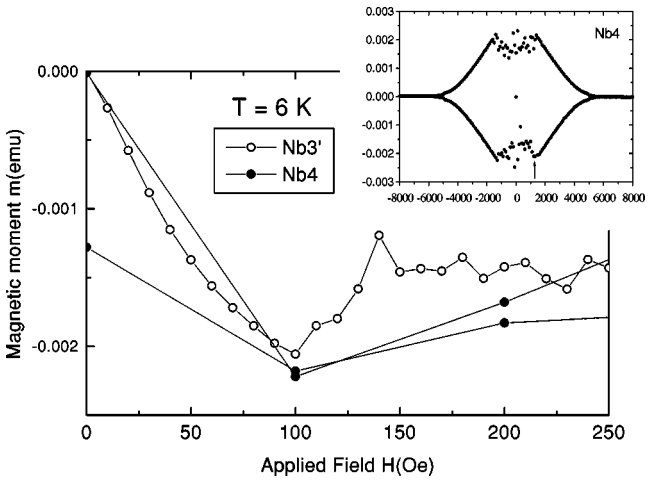

FIG. 1. Global magnetic moment as a function of applied field for samples Nb3′ (field step $\Delta H = 10$ Oe) and Nb4 ($\Delta H = 100$ Oe) at $T=6$ K. For sample Nb4 we show the first part of the loop in the ZFC state and also the last part of the loop increasing the field from the negative region. The whole hysteresis loop is shown in the inset. The arrow indicates the position of the SMP at $H = 1260$ Oe.

In Fig. 2, local measurements at a temperature $T = 5.83$ K similar as those of Fig. 1 and with a field step $\Delta H = 50$ Oe indicate that between 100 and 150 Oe an instability occurs which drives the flux into the middle of the sample (observed as the appearance of a nonzero field in sensors Nos. 2–5) decreasing the magnetization. Up to the second magnetization peak at $H_{SMP} \simeq 1300$ Oe, the instabilities are clearly observed. Note that the occurrence of the instabilities slows down the higher the applied field due to the decrease of the critical current density with field.

The lower the temperature, the larger is the instability effect and the larger is the flux entrance and the decrease of M. As an example we show in Fig. 3 the local magnetization

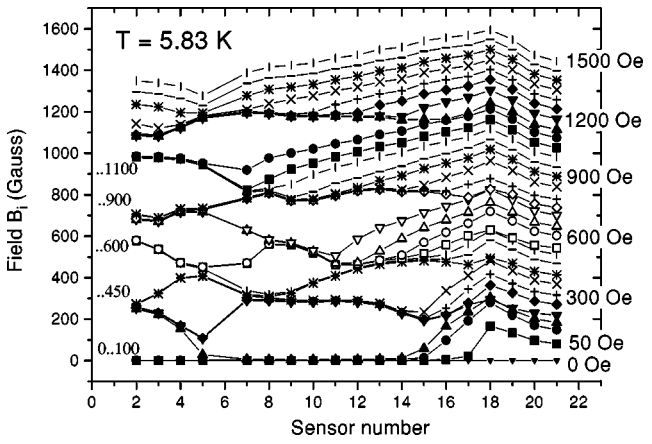

FIG. 2. Local field of sample Nb4 at $T=5.83$ K as a function of the sensor position. The middle of the sample is at the position 0 and the edge between sensors 18 and 19. The separation between the sensors is 20 μm. Each curve was obtained increasing the external field with a field step of 50 Oe from a zero-field-cooled state. The global second magnetization peak occurs at $H_{\mathrm{SMP}}\sim 1300$ Oe (see Fig. 1) and is characterized by a flux distribution (or critical current density) which crosses nearly half the width of the sample with constant slope [the points with the symbol $(\times)$ at the largest fields]. At higher fields a Bean-like profile is observed with a slope that decreases with field. The numbers at the left and in the figure indicate the field region in Oe where different flux profile lines overlap. For example, . . . 600 means that sensor 2 measured a similar local field at 500, 550, and 600 Oe applied fields.

data B_i-H measured by sensors $i=2-5$ at field steps $\Delta H=10$, 50, and 100 Oe and in Fig. 4 the corresponding flux distribution B_i obtained at $T=4.75$ K.

From both local and global measurements we conclude that the first magnetization peak $H_{fp}(T)$ is of the order of the field at which the first jump $H_{fj}(T)$ occurs. This behavior has been also recently observed in Bi2212 single crystals in a broad temperature range.[18]

A quantitative comparison between the values of H_{fj} obtained for the sample Nb4, for example, and those obtained from the available models [Eqs. (3) and (4)] is difficult because of the uncertainty in the values of the specific heat and j_c at a given field and temperature. However, a qualitative comparison is possible. Note that according to the adiabatic model (3) H_{fj} depends neither on the sweep rate nor on the sample thickness. On the other hand, within the more realistic model of Ref. 8, $H_{fj}\propto 1/(\dot{H}d^2)$ for ideal heat transfer or $H_{fj}\propto 1/(\dot{H}d)$ otherwise. Although in our measurements the field is changed step by step with a similar time interval between two adjacent applied fields, we approximate $\mu_0\Delta H/\Delta t\sim\dot{H}$. We note that in the SQUID measurements the time interval between field steps was similar to the rise time of the field, whereas in the μ-Hall measurements the rise time was smaller than the measuring time. In this case changing a factor of 2 the field step increases the defined $\dot{H}$ by a factor of ~ 1.7. Both kinds of measurements provided similar results. Our definition of the field sweep rate is similar to that used in published work where an experimental check for its consistency has been done.[3,5,21]

The results shown in Fig. 3 clearly demonstrate that H_{fj} is nearly independent of the sweep rate. This result is also confirmed at other temperatures. Moreover, the predicted thickness and sweep rate dependence [see Eq. (4)] appears also to be at odds with the experimental results shown in Fig. 1.

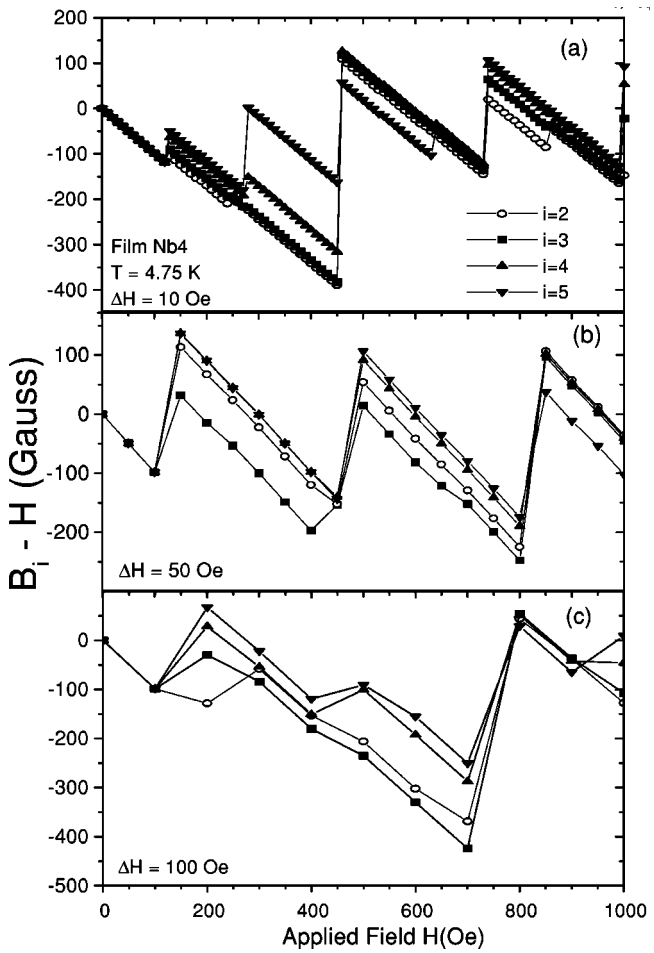

FIG. 3. Local magnetization at the position of the sensors 2–5 as a function of the applied field measured at different field steps ΔH for sample Nb4 and at $T=4.75$ K.

Note, however, that some details of the local field behavior depend indeed on the sweeping rate, as, for example, the number and amplitude of the jumps; see Fig. 3. It is expected that the variation of the external field acts as an instability-

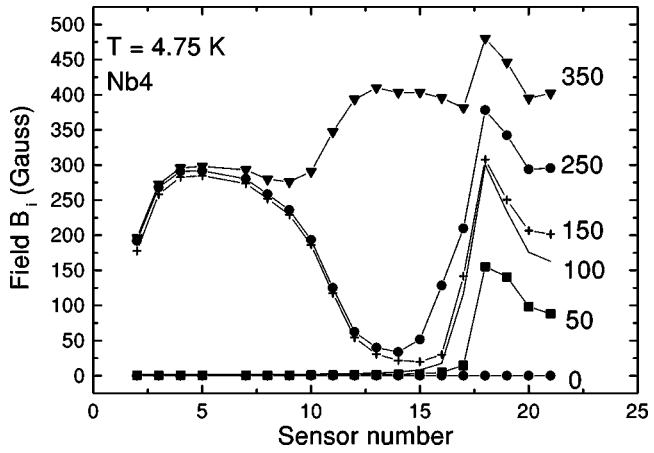

FIG. 4. Flux profile from the same data as in Fig. 3 obtained with a field step $\Delta H=50$ Oe.

driving perturbation. The experimental evidence on this influence remains still unclear. Measurements performed on $YBa_2Cu_3O_7$ HTS rings show a reduction of the number and amplitude of the magnetization jumps with a short-time magnetic cycling.[19] In some conventional superconductors both the independence of H_{fj} on the sweeping rate[20] and its growth at a high sweeping rate[3,21] were detected.

The theory of Ref. 8 assumes the modified Bean model for transverse geometry for the calculations of the flux profile. From our local results we observe that there is no Bean-like flux profile up to the SMP field; see Fig. 2. Moreover, the results show a remarkable effect, namely, that near H_{fj} the vortices penetrate the sample, forming a droplet with a dome shape far away from the film edges, i.e., near the center (see Fig. 4) or at the center of the sample (see Fig. 2), depending on the temperature. A further increase of the external field does not change homogeneously the flux profile inside the sample, but part of the vortices remain pinned. After a jump, the increase of field moves vortices from the edges and a Bean-like profile starts to develop; see Fig. 2. This development is stopped by new jumps. The higher the applied field, the lower the critical current density and therefore the larger is the penetration of the Bean-like profile into the sample.

It is interesting to note that domelike flux profiles at low enough fields have been already observed in platelet-shaped high-T_c crystals[22,23,14] due to the existence of a geometrical, surface or, in general, edge barrier given by the shape of the sample. The resulting field distribution with the specific dome-shaped profile is explained when, in the absence of bulk pinning, the vortex potential is minimized at the center of the sample. The finite thickness of the sample gives rise to a significant potential barrier close to the edges. The vortices, after crossing this barrier, are gathered into the center of the sample by the Lorenz force produced by the Meissner currents and form a droplet which spreads out with the field.

The observed domelike shape of the field profile at penetration fields of ~ 100 Oe (see Figs. 2 and 4), however, cannot be due to a surface barrier. Using torque magnetometry we have recently been able to measure the penetration field due to the geometrical barrier[24] for the sample Nb4. In this experiment the field is applied almost parallel to the main area of the film. The torque magnetometer device responds to the magnetization component perpendicular to the film main area. At low enough fields, the quite peculiar behavior of the measured magnetization as a function of applied field can be quantitatively interpreted by taking into account a geometrical barrier for the entrance of vortices.[24] According to the geometrical barrier model, the penetration field is given by $B_{gb} \simeq (4d/\pi w)^{0.5} B_{c1} \simeq 3.1$ Oe which nearly coincides with the penetration field of 3.4 Oe (given by the perpendicular applied field component) measured at $T = 5$ K.[24] Since the effect of the edge barrier to the flux profile in the sample vanishes at about 3 times the penetration field, the domelike profile observed in our Nb thin films at $\mu_0 H \gg B_{gb}$ cannot be explained by an edge barrier effect.

The absence of a Bean-like profile in our thin films at fields close to the first flux jump field is probably one of the reasons for the failure of the instability criterion given by Eq. (4). It is tempting to speculate that irregularities at the edges of the thin films are preferred channels for the entrance of vortices in the sample. However, the observed strong temperature dependence of the flux profile at H_{fj} (see Figs. 2 and 4) speaks for the influence of a thermomagnetic instability. Also, as we will see in the next section, we have observed similar behavior near H_{fp} for samples with identical thickness but which have been patterned differently, as well as for a sample in which the edges have been cut with a diamond saw.

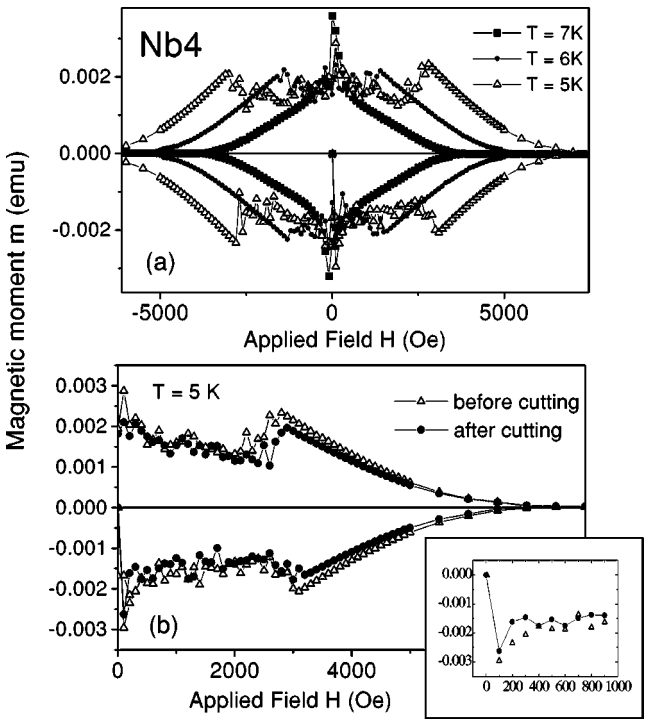

FIG. 5. (a) Magnetization hysteresis loops of sample Nb4 measured with the SQUID at three different temperatures. (b) Positive field region of the magnetization hysteresis loops for the same sample before and after cutting the edges with a diamond saw. The inset is a blow up of the region near H_{fj}.

B. Second magnetization peak

In this section we show and discuss the temperature and sample dependence of the SMP. Figure 5(a) shows the magnetization hysteresis loops performed on sample Nb4 at different temperatures. The observed behavior is similar to that reported previously for the Nb0 sample.[13] In a zero-field-cooled state the absolute magnetization increases. After reaching the first magnetization maximum, it decreases, showing a jumping behavior. These jumps remain up to a field where the magnetization shows a second maximum, i.e., the SMP. We found a very good agreement between the values of the field at which the SMP develops obtained from global and local measurements.

In order to check whether the SMP depends on the characteristics of the edges of the film we have measured the sample Nb4 before and after cutting its edges with a diamond saw. The volume change due to this cutting was $\sim 5\%$. The results are shown in Fig. 5(b). Within the error of the measurement no appreciable difference in the field position H_{SMP} is observed. Differences of the order of $\sim 10\%$ in $H_{SMP}(T)$ are observed, however, between the samples struc-

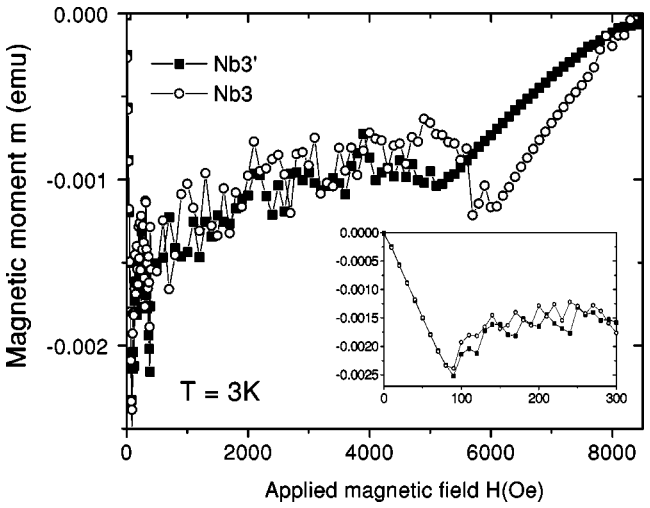

FIG. 6. Magnetic moment as a function of applied field for samples Nb3 and Nb3′ and at 3 K. The inset is a blow up of the region at the first magnetization peak for both samples.

tured with different methods. As an example, we show in Fig. 6 the SMP for samples Nb3 and Nb3′ which were patterned using the ''lift-off'' and chemical etching methods, respectively. The $H_{SMP}(T)$ of sample Nb3 is larger than that of Nb3′. This difference is also observed for samples Nb1 and Nb9 which have similar thickness. This difference is attributed to different critical current densities j_c.

As discussed in the last section, one may speculate that $H_{fp}(\simeq H_{fj})$ depends on the characteristics of the edges. This is not observed experimentally, neither after cutting nor for samples patterned differently; see inset in Fig. 6.

According to the classical theory, for a given critical current density the geometry of the sample plays an important role for the existence of TMI's. Indeed, the SMP vanishes at a given temperature for the Nb3s sample which consists of nine stripes of 95 μm each, obtained structuring sample Nb3. These results are shown in Fig. 7.

Using Eqs. (1) and (3) the TMI criterion can be written as

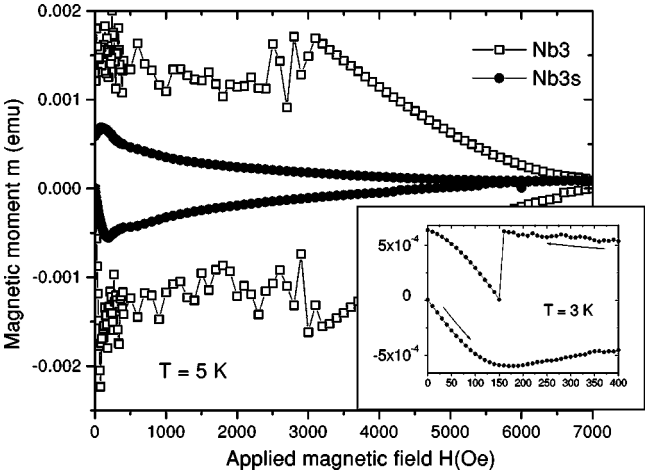

FIG. 7. Positive field region of the magnetization hysteresis loops for sample Nb3 and after its structuring in nine stripes, sample Nb3s, at 5 K. The inset shows part of the hysteresis loop of sample Nb3s at 3 K.

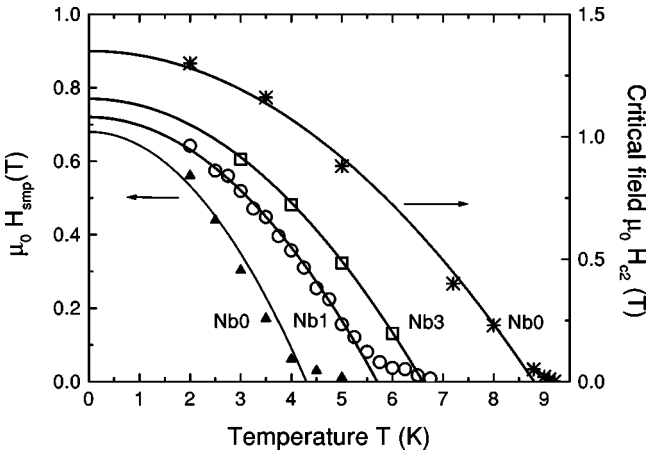

FIG. 8. Temperature dependence of the second magnetization peak field $H_{SMP}(T)$ of samples Nb0, Nb1, and Nb3. The upper critical field measured for sample Nb0 is also shown. The solid lines follow the function $H_0(1-t^2)$ with $t=T/T_0$ for H_{SMP} or $t \sim T/T_c$ for H_{c2}. H_0 and T_0 are parameters obtained from the fits.

$$s_{\rm crit} \simeq \frac{10 H_{fp}}{4\pi j_c}. \tag{5}$$

From the measurements we obtain $H_{fp} \sim 100$ Oe and $j_c \sim 10^{10}$ A/m^2. With these values we estimate a critical effective size $s_{\rm crit} \leqslant 1$ μm. Taking into account that we apply the field perpendicular to the sample main surface, the effective sample geometry s to compare with is given by Eq. (2). From this equation we obtain that $s \geqslant 6$ μm, taking into account the geometry of the films. This indicates that even in a 95 μm width sample and according to the instability criterion, one should observe flux jumps at low enough temperatures. Indeed, we start observing flux jumps in the NB3s sample at $T \leqslant 3.5$ K. In the inset of Fig. 7 we note tiny magnetization jumps at $H > 200$ Oe in the increasing and decreasing field part of the loop where we also observe a large jump at $H \simeq 150$ Oe at 3 K. We note also that the jumpy magnetization behavior at $H < H_{SMP}(T)$ measured in the wider film Nb3, transforms actually in a rather flat and smooth ''hollow'' in $M(H)$ in the Nb3s sample. The SMP feature is therefore hardly recognized at ~ 500 Oe; see Fig. 7.

Figure 8 shows the temperature dependence of H_{SMP} for some of the measured samples as well as the upper critical field $H_{c2}(T)$ for the sample Nb0. Within the error in the determination of $H_{c2}(T)$ from the hysteresis loops using the reversibility criterion, $H_{c2}(T)$ is sample independent. This is not the case for $H_{SMP}(T)$ as the results in Fig. 8 indicate. The thinner the thin film, the lower is the $H_{SMP}(T)$. The results also indicate that $H_{SMP}(T)$ shows a similar temperature dependence as $H_{c2}(T)$.

In order to characterize roughly the geometry dependence of $H_{SMP}(T)$ we fit its temperature dependence using the equation $H_{SMP}(T)=H_0(1-t^2)$ with H_0 a free parameter and $t=T/T_0$. We neglect the positive curvature observed for $H_{SMP}(T)$ as well as for $H_{c2}(T)$ at high enough temperatures. We take the shift of T_0 as a criterion for the shift of $H_{SMP}(T)$ with geometry. In Fig. 9 we show the effective size dependence of T_0. Roughly, it increases linearly with s with a tendency to show a negative curvature at large s val-

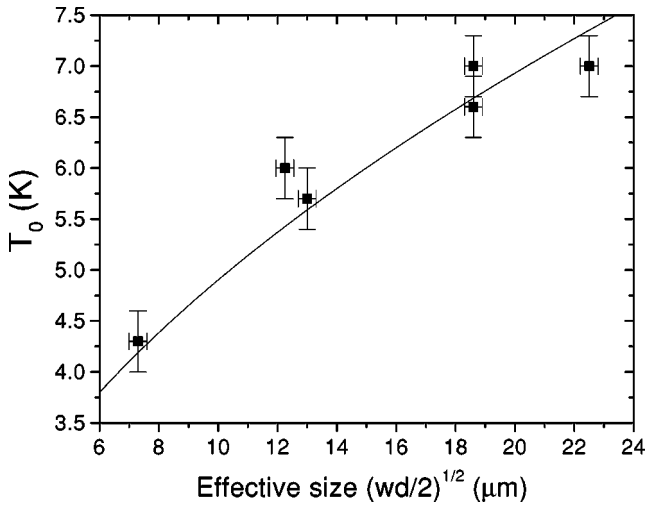

FIG. 9. Extrapolated temperature T_0 from the fits of $H_{SMP}(T)$ (see Fig. 8) as a function of the effective geometrical size $s=(wd/2)^{0.5}$. The solid line is given by $1.55\,s^{0.5}\,\mathrm{K}/\mu\mathrm{m}^{0.5}$.

ues. If we take $T_0=0$ K at $s=0$ as a fixed point, then the observed dependence can be fitted with a square root function of s as shown in Fig. 9. Although this result has to be considered as empirical, it can be roughly obtained from Eq. (1) if we assume $C\sim T^3$ and $j_c(T)\sim 1-(T/T_c)$. As noted above, we stress that a quantitative estimate is difficult because $j_c(T)$ cannot be determined in the region of TMI's and also it is unclear which effective value (between the values for the Nb film and that one for the substrate) for the specific heat has to be used.

The local and global measurements reveal that the SMP occurs when the critical current density reaches a sample-dependent value which is roughly temperature independent, i.e., $j_c(H=H_{SMP})=j_{c0}\sim$const. This is shown in Fig. 10 for three different samples. The critical current density has been calculated from the width of the magnetization loops at $H=H_{SMP}$, i.e., $j_c(H)=[4/w(1-w/3l)]|M_{hw}(H)|$ (Ref. 16) (for length $l>w$) and the half-width of the hysteresis loop $|M_{hw}(H)|=(1/2)[M^+(H)-M^-(H)]$ (M^+ and M^- are the magnetization corresponding to the ascending and descending branches of the hysteresis loop, respectively). This result implies that the TMI is strongly suppressed when the gradient of the vortex distribution in the sample ($\propto j_c$) decreases below a certain value. The rather small increase of $j_c(H_{SMP})$ with temperature (see Fig. 10) can be understood by taking the classical approximation

$$j_c(h)=\frac{c_0}{h+h_0},\quad h=\frac{H}{H_{c2}(T)},\tag{6}$$

and $H_{SMP}(t_1)=H_{SMP}(0)(1-t_1^2)$, $H_{c2}(t_2)=H_{c2}(0)(1-t_2^2)$, with $t_1=T/T_0$ and $t_2=T/T^*$,$(T^*\sim T_c)$ (see Fig. 8); c_0 and h_0 are free parameters. The temperature dependence of H_{SMP} is then given by $H_{SMP}(T)\sim[(c_0/j_{c0})-h_0]H_{c2}(T)$; i.e., it reflects roughly the temperature dependence of H_{c2}.

V. CONCLUDING REMARKS

In this work we studied flux-jump instabilities in Nb thin films by means of global magnetization $M(H)$ and local field

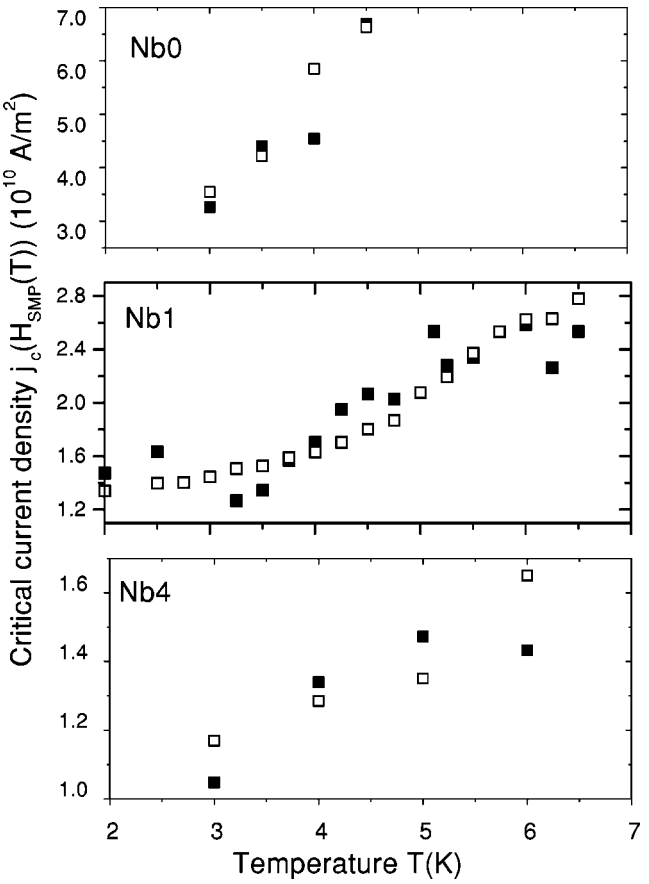

FIG. 10. Solid symbols: temperature dependence of the critical current density at the second magnetization peak for three samples. Open symbols are calculated using $j_c(h(T))=c_0/\{[H_{SMP}(T)/H_{c2}(T)]+h_0\}$, with c_0 and h_0 as free parameters.

$B_i(H,x)$ measurements using SQUID and μ-Hall sensors, respectively. Large jumps in both $M(H)$ and $B_i(H)$ as well as pronounced irregularities of large scale gradients in the vortex density take place at sufficiently low temperatures and at low applied magnetic fields. The location of the $H_{SMP}(T)$ boundary in the H-T plane, which separates jumpylike from predominantly continuous M vs H and B_i vs H behavior, depends on the effective film size $s\sim(wd/2)^{1/2}$.

At low enough fields but larger than H_{fj}, the reduction of the absolute irreversible magnetization relative to the isothermal critical state value can be understood as due to local heating which leads to the second magnetization peak feature at the field $H_{SMP}(T)>H_{fj}$. At $H\geqslant H_{SMP}$ the isothermal critical state is reestablished.

It is also shown in this work that magnetization jumps become smaller in magnitude or even vanish with a reduction of the film size. These findings as well as the observed dependence of the amplitude and number of flux jumps on the field sweeping rate dH/dt (Refs. 13 and 25) provide the experimental evidence for the TMI origin of the SMP.

Within the developed theories of the thermomagnetic instability a rapid variation of the applied magnetic field is expected to act as the instability-driving perturbation such that H_{fj} should decrease with increasing the field sweeping rate dH/dt.[3,8,21] Thus, the near independence of H_{fj} on the sweeping rate observed in the present work remains to be explained. We note also that even an increase of H_{fj} at high

sweeping rates was detected in some superconductors.[3,21] It has been suggested[3,21] that a nonuniform heating may be responsible for such an effect. However, theoretical understanding of the TMI's at such conditions is still lacking.

Another striking result of our studies is the observation of a dome-shaped flux profile at $H<H_{SMP}(T)$. At high enough temperatures and/or applied fields $[H>H_{SMP}(T)]$ the Bean-like profile is recovered. Domelike flux profiles have been also measured in Bi2212 crystals and attributed to edge barriers.[14,22,23] The results of this work demonstrate that dome profiles can also arise from a TMI effect.

In general and due to the influence of the giant vortex creep, the magnetization data in HTS crystals do not show clear noisy behavior. We note, however, that recently performed magnetization measurements in Bi2212 crystals show pronounced jumps of the irreversible magnetization.[18] These jumps as well as the second magnetization peak in Bi2212 vanish simultaneously when the crystal size is reduced. In spite of the similarities with the results in Nb presented here, we stress that the underlying mechanisms which trigger the magnetic instabilities may be different for these superconductors.

ACKNOWLEDGMENTS

This study was supported by the Deutsche Forschungsgemeinschaft under ''Phänomene an den Miniaturisierungsgrenzen'' (DFG IK 24/B1-1, project H) and by the German-Israeli Foundation for Scientific Research and Development (Grant No. G-553-191.14/97). We gratefully acknowledge the assistance of Youri Myasoedov from the Weizmann Institute.

*Present address: Quantum Institute, University of California, Santa Barbara, CA 93106.

[1] C. P. Bean, Rev. Mod. Phys. **36**, 41 (1964).
[2] P. S. Swartz and C. P. Bean, J. Appl. Phys. **39**, 4991 (1968).
[3] For a review see R. G. Mints and A. L. Rakhmanov, Rev. Mod. Phys. **53**, 551 (1981), and references therein.
[4] For a recent paper see E. R. Nowak, O. W. Taylor, L. Liu, H. M. Jaeger, and T. I. Selinder, Phys. Rev. B **55**, 11 702 (1997).
[5] M. E. McHenry, H. S. Lessure, M. P. Maley, J. Y. Coulter, I. Tanaka, and H. Kojima, Physica C **190**, 403 (1992).
[6] A. Gerber, J. N. Li, Z. Tarnawski, J. J. M. Franse, and A. A. Menovsky, Phys. Rev. B **47**, 6047 (1993).
[7] K.-H. Müller and C. Andrikidis, Phys. Rev. B **49**, 1294 (1994).
[8] R. G. Mints and E. H. Brandt, Phys. Rev. B **54**, 12 421 (1996).
[9] M. Guillot, M. Potel, P. Gougeon, H. Noel, J. C. Levet, G. Chouteau, and J. L. Tholence, Phys. Lett. A **127**, 363 (1988).
[10] K. Rogacki, P. Esquinazi, E. Faulhaber, and W. Sadowski, Physica C **246**, 123 (1995).
[11] N. H. Zebouni, A. Venkataren, G. Rao, C. Grenier, and J. Reynolds, Phys. Rev. Lett. **13**, 606 (1964).
[12] K. Behnia, C. Capan, D. Mailly, and B. Etienne, cond-mat/9902334 (unpublished).
[13] Y. Kopelevich and P. Esquinazi, J. Low Temp. Phys. **113**, 1 (1998).
[14] D. Majer, E. Zeldov, H. Shtrikman, and M. Konzcykowski, in *Coherence in High-Temperature Superconductors*, edited by G. Deutscher and A. Revcolevschi (World Scientific, Singapore, 1996), p. 271.
[15] E. Zeldov, D. Majer, M. Konczykowski, V. Geshkenbein, and V. Vinokur, Nature (London) **375**, 373 (1995).
[16] This results from the fact that the field shielded at the sample center is $j_c d$ instead of $j_c w$. See, for example, H. Wiesinger *et al.*, Physica C **272**, 79 (1996); M. Däumling and D. Larbalestier, Phys. Rev. B **40**, 9350 (1989).
[17] A. Pan, M. Ziese, R. Höhne, P. Esquinazi, S. Knappe, and H. Koch, Physica C **301**, 72 (1998).
[18] Y. Kopelevich, S. Moehlecke, J. H. S. Torres, R. Ricardo da Silva, and P. Esquinazi, J. Low Temp. Phys. **116**, 261 (1999).
[19] C. E. Gough, Int. J. Mod. Phys. B **1**, 891 (1987).
[20] R. B. Harrison, J. P. Pendrys, and L. S. Wright, J. Low Temp. Phys. **18**, 113 (1975).
[21] S. L. Wipf, Cryogenics **31**, 936 (1991).
[22] M. V. Indenbom *et al.*, in *Critical Currents in Superconductors*, edited by H. W. Weber (World Scientific, Singapore, 1994), p. 327; Physica C **222**, 203 (1994).
[23] E. Zeldov, A. Larkin, V. Geshkenbein, M. Konczykowski, D. Majer, B. Kheykovich, V. Vinokur, and H. Shtrikham, Phys. Rev. Lett. **73**, 1428 (1994).
[24] A. Pan, R. Höhn, M. Ziese, P. Esquinazi, and C. Assmann, in *Physics and Material Sciences of Vortex States, Flux Pinning and Dynamics*, edited by R. Kossowsky *et al.* (Kluwer Academic, Dordrecht, 1999), p. 545.
[25] P. Esquinazi, R. Höhne, Y. Kopelevich, A. Pan, and M. Ziese, in *Physics and Material Sciences of Vortex States, Flux Pinning and Dynamics* (Ref. 24), p. 149.